SANDIA REPORT
SAND2017-13270
Unlimited Release
Printed September 2017

Smart Grid R&D SSM KIER FY17 Report

Marvin Cook
David Wilson

Prepared by
Sandia National Laboratories
Albuquerque, New Mexico 87185 and Livermore, California 94550

Sandia National Laboratories is a multimission laboratory managed and operated by National Technology and Engineering Solutions of Sandia, LLC, a wholly owned subsidiary of Honeywell International, Inc., for the U.S. Department of Energy's National Nuclear Security Administration under contract DE-NA0003525.

Issued by Sandia National Laboratories, operated for the United States Department of Energy by National Technology and Engineering Solutions of Sandia, LLC.

Available to DOE and DOE contractors from
U.S. Department of Energy
Office of Scientific and Technical Information
P.O. Box 62
Oak Ridge, TN 37831

Telephone: (865) 576-8401
Facsimile: (865) 576-5728
E-Mail: reports@osti.gov
Online ordering: http://www.osti.gov/scitech

Available to the public from
U.S. Department of Commerce
National Technical Information Service
5301 Shawnee Rd
Alexandria, VA 22312

Telephone: (800) 553-6847
Facsimile: (703) 605-6900
E-Mail: orders@ntis.gov
Online order: https://classic.ntis.gov/help/order-methods/

SAND201X-XXXX
Printed September 2017
Unlimited Release

Smart Grid R&D SSM KIER FY17 Report

Marvin Cook
Military & Energy Systems Analysis

David Wilson
Electrical Science & Experiments

Sandia National Laboratories
P. O. Box 5800
Albuquerque, New Mexico 87185-MS1108

Abstract

This report summarizes collaborative efforts between Secure Scalable Microgrid and Korean Institute of Energy Research team members. The efforts aim to advance microgrid research and development towards the efficient utilization of networked microgrids. The collaboration resulted in the identification of experimental and real time simulation capabilities that may be leveraged for networked microgrids research, development, and demonstration. Additional research was performed to support the demonstration of control techniques within real time simulation and with hardware in the loop for DC microgrids.

ACKNOWLEDGMENTS

This work was funded by the U.S. Department of Energy Office of Electricity Delivery and Energy Reliability.

TABLE OF CONTENTS

NOMENCLATURE

Abbreviation	Definition
SSM	Secure Scalable Microgrid
KIER	Korean Institute of Energy Research
HIL	Hardware in the loop
MOTIE	Ministry of Trade, Industry, and Energy
DOE	U.S. Department of Energy
OE	Office of Electricity Delivery and Energy Reliability

1. INTRODUCTION

In support of DOE's International Affairs' Asia Pacific Energy Consortium, DOE is interested in coordinating collaborative advanced microgrid design efforts with their counterpart in Korea, MOTIE. To support that effort, DOE/OE has agreed to fund Sandia to work with the KIER Research to initiate an advanced microgrid evaluation and conceptual design at the KNA in Jinhae. Jinhae is a naval base in southern Korea that is also shared by the US Navy. Since the KNA shares the same energy infrastructure with the US Navy, DOE and MOTIE believe that these efforts between Sandia, KIER, and the KNA will help accelerate future microgrid research, development, and demonstration projects between MOTIE and other Korean research agencies, DOE, and the US Navy in the future.

The overall goal is to collaborate to develop and utilize microgrid analysis and design approaches and tools to support the design, implementation, and operation of microgrids at military installations in Korea to improve energy security, reliability, and resiliency. The range of activities include the development of design and analysis tools and protocols, development of operation protocols, and establishment of operational testing protocols for microgrid verification and validation. In FY17, Sandia collaborated with KIER to identify research facilities with hardware and simulation capabilities that may be leveraged for future microgrid RD&D. Additional efforts focused on the evaluating KNA campus microgrids through real time simulation and hardware in the loop representations. This report summarizes these FY17 efforts and resultant findings.

2. RESEARCH FACILITIES

SNL and KIER reviewed existing research facilities with hardware, modeling, and simulation capabilities relevant to networked microgrid RD&D. The organizations share several common approaches and capabilities that may be leveraged for future networked microgrid RD&D. The facilities with hardware capabilities span tens of kW to utility scale installations. The organizations identified common modeling and simulation efforts that include MATLAB, Simulink, and Opal-RT programming. Utilization of the research facilities and capabilities for evaluating various networked microgrid topologies and scales requires further coordination between the organizations to appropriately characterize use case scenarios. The identified capabilities have been further summarized in a presentation format as part of the project deliverables [1,2].

3. SYSTEM MODELING

KNA campus data acquisition system captures power consumption measurements at multiple building points of interest [refer to Appendix A]. KIER provided a KNA data set with one year of measurements at 6 second intervals. In addition to the this data acquisition information, KIER provided hotel service load information for two ships at 10 second intervals. SNL reviewed the data sets to correct any missing or corrupt data points and identify timespans of interest. The SNL controls team identified half hour intervals that captured the most significant load demand swings.

SNL has been working with Michigan Tech University's microgrid team for the past five years to effectively model microgrid systems. The effort has resulted in a modeling engine that can auto-generate detailed MATLAB Simulink and Opal RT software representations based on spreadsheet style specifications. This modeling capability was leveraged and further refined to meet the KNA campus modeling needs.

SNL developed a reduced order model (ROM) representation of the KNA campus microgrid system. The ROM aims to capture the pertinent performance characteristics of the detailed system model representation. Control algorithms may be evaluated and refined against the ROM representation, supporting transition to real time physical and simulated environments.

4. CONTROL DESIGN

The baseline summarized for this discussion utilizes a networked microgrid system consisting of three modules tied together with an AC ring bus to supply power to servicing hotel loads for land or sea based applications.

4.1. Reduced Order Model (ROM) Networked Mobile Microgrid Model

This section summarizes ROM development that captures the essence of a more detailed networked microgrid system with real-time implementation being the final goal for the control system. Functionally, the baseline system can be represented in Figure 1 where each individual module retains the simplified characteristics consisting of; i) source/storage, ii) bus storage, iii) DC boost converters, iv) DC/AC converters, v) a connection to the other modules through an AC ring bus, and vi) AC service loads.

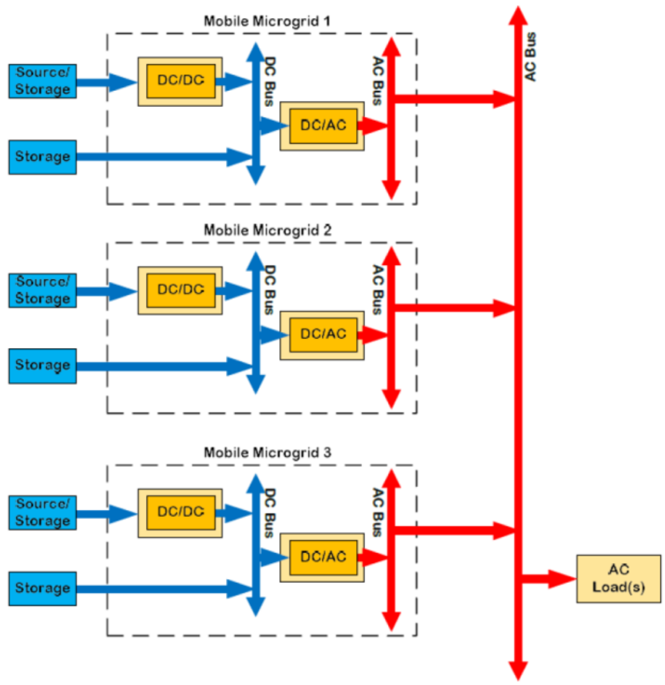

Figure 1. Three Networked Mobile Microgrid Schematic

To develop the dynamical governing equations for the ROM several assumptions are made; i) the diesel engine dynamics are ignored and replaced by a DC source, storage device and boost converter. ii) The battery and DC/DC converter are modeled as a DC current injection storage device. iii) The inverter is modeled as a loss-less power balance between DC and DQ. iv) The lines of the AC ring-bus are sufficiently short to ignore the line dynamics and model the ring as a single AC bus.

The full system dynamical ROM can be summarized in matrix form as

$$M\dot{x} = Rx + f(x,u,t) + D^T v + B^T u = \left[\overline{R} + \widetilde{R}\right]x + f(x,u,t) + D^T v + B^T u$$

where the state, controls, an input vectors are defined as

$\underline{x}^{T} = \{i_{s,1}(t), v_{dc,1}(t), i_{d,1}(t), i_{q,1}(t), i_{s,2}(t), v_{dc,2}(t), i_{d,2}(t), i_{q,2}(t), i_{s,3}(t), v_{dc,3}(t), i_{d,3}(t), i_{q,3}(t), v_{dB}(t), v_{qB}(t)\}$

$\underline{u}^{T} = \{u_{s,1}, u_{s,2}, u_{s,3}, u_{dc,1}, u_{dc,2}, u_{dc,3}, u_{dB}, u_{qB}\}$

$\underline{v}^{T} = \{v_{s,1}, v_{s,2}, v_{s,3}\}$

with the detailed development give in [3-8].

4.2. Networked Microgrid HSSPFC Control Design

The R matrix is decomposed further as the sum of a diagonal and skew-symmetric matrix components. The M matrix consists of the inductance and capacitance elements of the circuit and the R matrix consists of the resistive elements of the circuit. The v-vector consists of the general source inputs to the network and the u-vector contains the controller inputs. The state x is composed of the circuit currents and bus voltage, respectively. The error state along with the reference control are defined as

$$e = \tilde{x} = x_{ref} - x$$
$$M\dot{x}_{ref} = \left[\bar{R} + \tilde{R}\right]x_{ref} + D^T v + B^T u_{ref}.$$

It is assumed that the reference state vector is constant, e.g., operating at some desired steady-state condition, and the reference control signal becomes

$$B^T u_{ref} = -\left[\bar{R} + \tilde{R}\right]x_{ref} - D^T v \tag{1}$$

Next, based on the error-state the Hamiltonian or energy surface is defined as

$$H = \frac{1}{2}\tilde{x}^T M\tilde{x} + \frac{1}{2}\left(\int \tilde{x}\,dt\right)^T B^T K_I B\left(\int \tilde{x}\,dt\right) \quad \forall \quad \tilde{x} \neq 0$$

where the controller integral term provides a control potential energy to help design or shape the energy surface to meet the static stability condition. Note the integral controller diagonal gain matrix is positive definite.

The Hamiltonian time derivative (or power flow) becomes:

$$\dot{H} = \tilde{x}^T M\dot{\tilde{x}} = \tilde{x}^T\left[M\dot{x}_{ref} - M\dot{x}\right] + \tilde{x}^T B^T K_I B\int \tilde{x}\,dt$$
$$\dot{H} = \tilde{x}^T \bar{R}\tilde{x} + \tilde{x}^T \Delta u + \tilde{x}^T B^T K_I B\int \tilde{x}\,dt$$

where the skew-symmetric portion of the R matrix is zero and the feedback controller is determined by

$$\Delta u = u_{ref} - u.$$

In the next step, a Proportional-Integral (PI) controller is proposed as

$$\Delta u = -K_P B\tilde{x} - K_I B\int \tilde{x}\,dt. \tag{2}$$

Substituting and simplifying the Hamiltonian time derivative (power flow) yields

$$\dot{H} = -\tilde{x}^T \left[B^T K_P B - \overline{R}\right]\tilde{x} < 0$$

which is the dynamic stability condition. Performance is determined by the selection of the proportional controller diagonal gain matrix, defined as positive definite.

The HSSPFC design is composed of both feedforward and feedback portions. The feedback controller design integrates the energy storage into the network microgrid. It includes both the feedback into the guidance command algorithm for the boost converter duty cycles and implements the energy storage systems. The duty cycle servo control is fully coupled and the HSSPFC for the energy storage is decoupled due to the skew-symmetric form of the R matrix.

4.3. Energy Management and Optimization

SNL has developed a multi-agent system architecture for energy management of single and networked microgrids.

4.3.1. Software Agents

The software agents' main responsibilities include reading measurement signals from the energy system, updating the system status model, performing logic to determine appropriate control signals, and sending controls signals to the energy system. Software agents achieve automation by applying a SENSE-DECIDE-ACT cycle at a frequency that satisfies system objectives, see Figure 2.

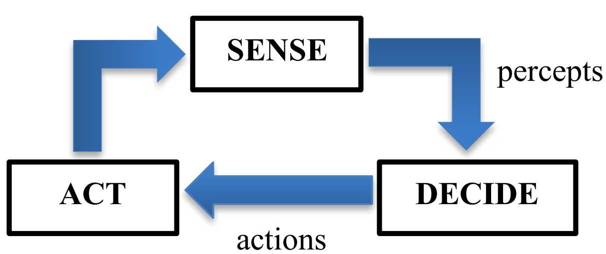

Figure 2. Agent Monitor and Control Loop

A single agent is responsible for managing and representing a single microgrid module. Each agent may share local microgrid status information and request power support from neighboring microgrids through peer agents.

The control effort may leverage ideal energy storage system that can provide power, energy storage, and frequency response requirements for a networked microgrid system. The control architecture supports evaluation of scenarios that trade-off physical energy storage metrics with information flow metrics through optimization. The control design has been designed to be implemented in the Matlab/Simulink or OPAL-RT real-time environments.

4.3.2. Optimization

A dynamic optimization (Optizelle) formulation has been developed to accommodate a large number of generation, loads, busses, and energy storage resources [9]. The formulation allows minimization of the change in the boost converter duty cycle, the amount of storage used by the microgrid, the parasitic losses, or the amount of power. Constraints are then applied to the formulation by the circuit equations for the microgrid, discretization in time, and by bounds on each individual parameter.

The optimization problem setup for multiple or networked microgrids contains the following performance index to be minimized

$$
\begin{aligned}
&\tfrac{1}{2}\left(\|w_{A_{duty}}\dot{\lambda_A}\|^2 + \|w_{E_{duty}}\dot{\lambda_E}\|^2\right) + \\
&\tfrac{1}{2}\left(\|w_{A_{control}}u_A u_{A_{switch}}\|^2 + \|w_{B_{control}}u_B u_{B\,switch}\|^2 + \|w_{F_{control}}u_{F_d}u_{F\,switch}\|^2 + \|w_{F_{control}}u_{F_q}u_{F\,switch}\|^2\right) + \\
&\tfrac{1}{2}\left(\langle w_{A_{loss}}R_A i_A, i_A\rangle + \langle w_{E_{loss}}R_E i_{E_d}, i_{E_d}\rangle + \langle w_{E_{loss}}R_E i_{E_q}, i_{E_q}\rangle\right) \\
&\tfrac{1}{2}\left(\|w_{A_{power}}\dot{e_A}u_{switch}\|^2 + \|w_{B_{power}}\dot{e_B}u_{B\,switch}\|^2 + \|w_{F_{power}}\dot{e_{F_d}}u_{F\,switch}\|^2 + \|w_{F_{power}}\dot{e_{F_q}}u_{F\,switch}\|^2\right)
\end{aligned}
$$

Subject to; boost converters, DC buses, AC to DC connectors, AC buses, inverters, trigonometric constraints, power limits, discretization, and parameter bounds.

For the KNA campus project, the optimizer aims to apply a control methodology that allows for the reduction of nonrenewable resources while still meeting the critical load demands.

The microgrid includes the following components:

- Two 15 kW generators running at 480 ± 10% V
- DC bus running at 720 ± 10% V
- One resistive load on DC bus begins at 10 kW, transitions to 20 kW, back to 10 kW, and finally back to 20

The optimal control formulation models two boost converters tied to a DC bus as described in Figure 3 and 4.

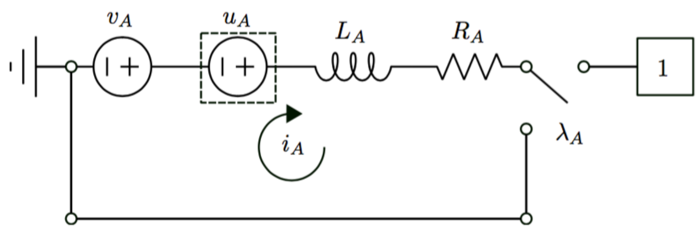

Figure 3. Boost Converter

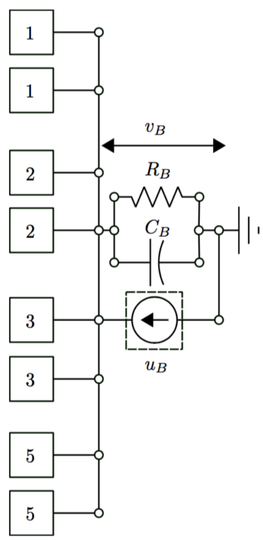

Figure 4. DC Bus

5. CONTROL RESULTS

5.1. Optimization

SNL has developed a multi-agent system architAn optimal control methodology was applied to reduce the dependence on generators that use nonrenewable resources. Depending on the load demands placed on the microgrid, there may not be an ability to completely eliminate nonrenewable resource usage, but with an appropriate storage device, usage may be significantly reduced.

The KNA campus microgrid was modeled with two 15 kW generators running at 480 ± 10% V attached to a DC bus running at 720 ± 10% V. A resistive load on the DC Bus begins with a load demand of 10 kW, transitions to 20 kW, then to 10 kW, and finally to 20 kW. The optimization analysis focused on evaluating how the control reacts to predictably changing loads, while reducing the change in the boost converter duty cycle. Energy storage on the DC bus was used to compensate for the changes in boost converter duty cycles. The optimal control methodology successfully minimized the change in boost converter duty cycles, see Figures 5-10.

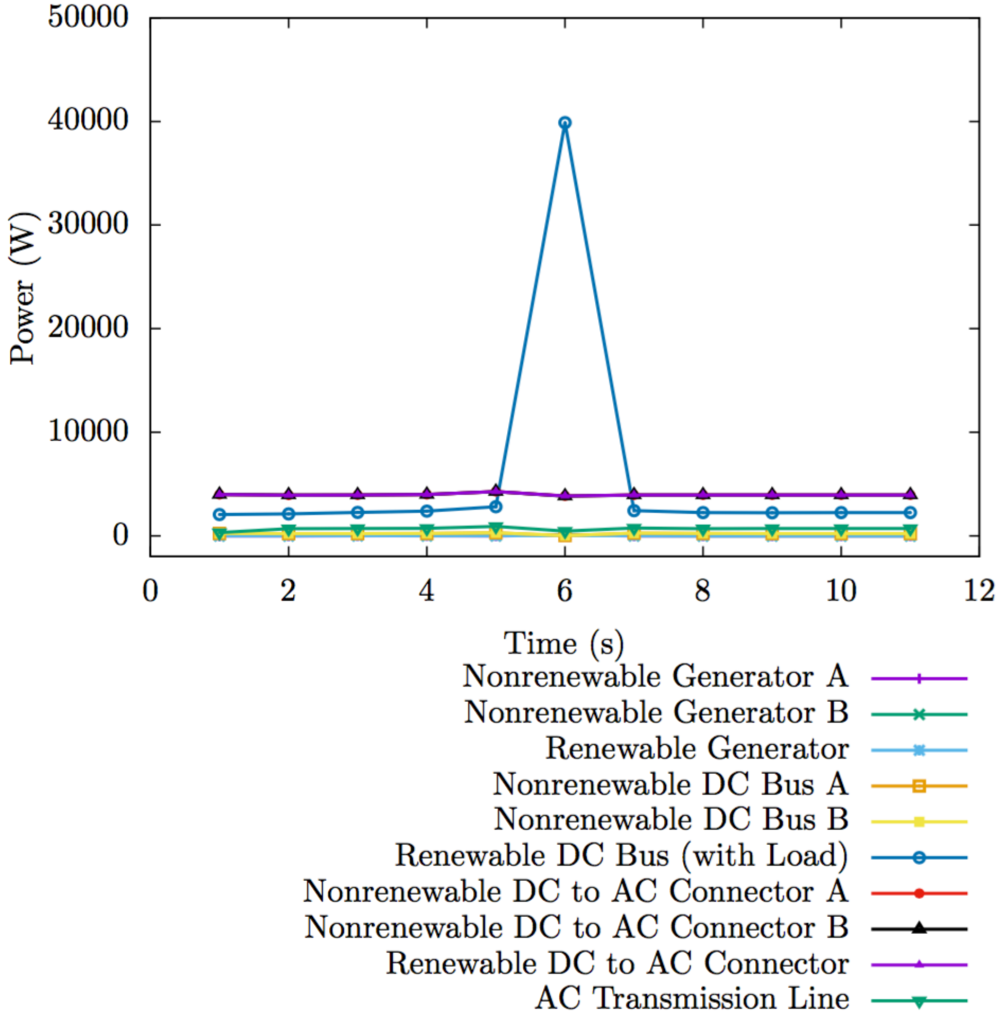

Figure 5. Power Consumed by Load

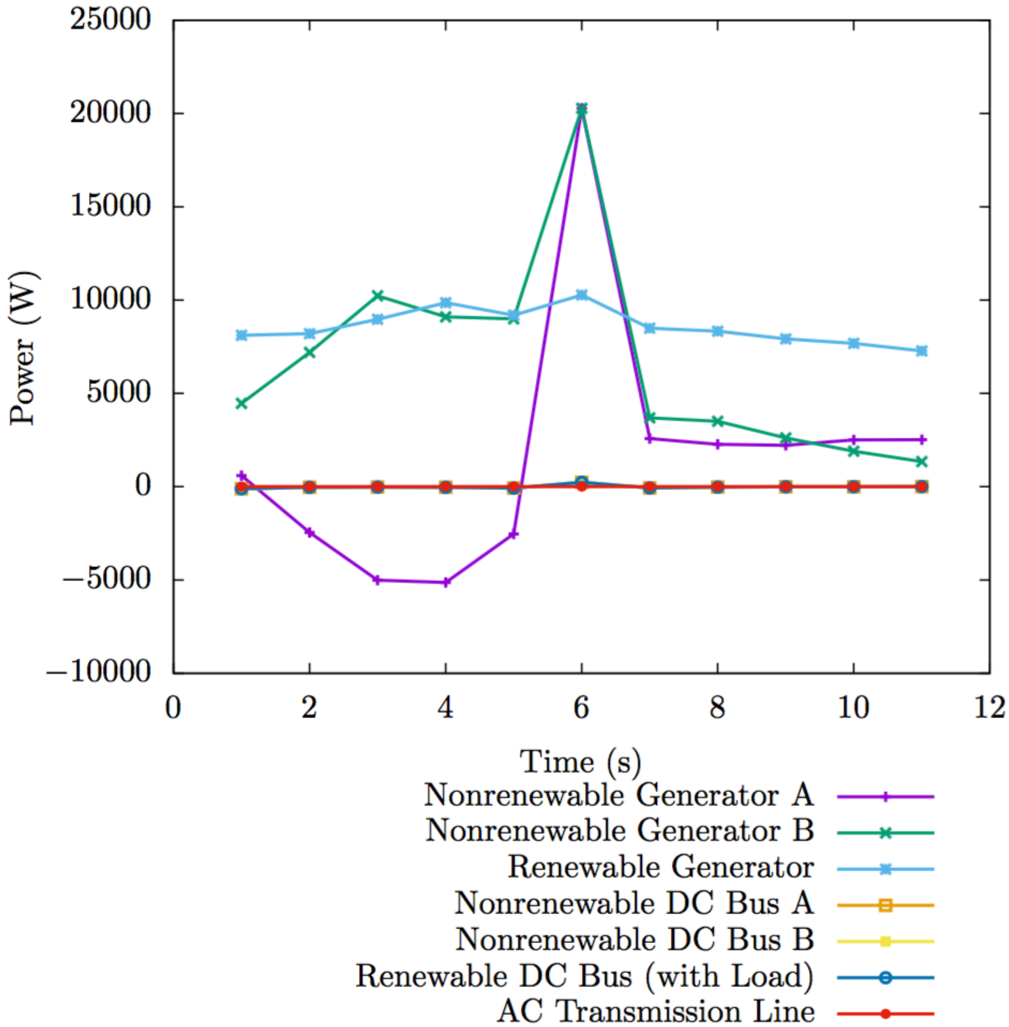

Figure 6. Power generated by microgrid components

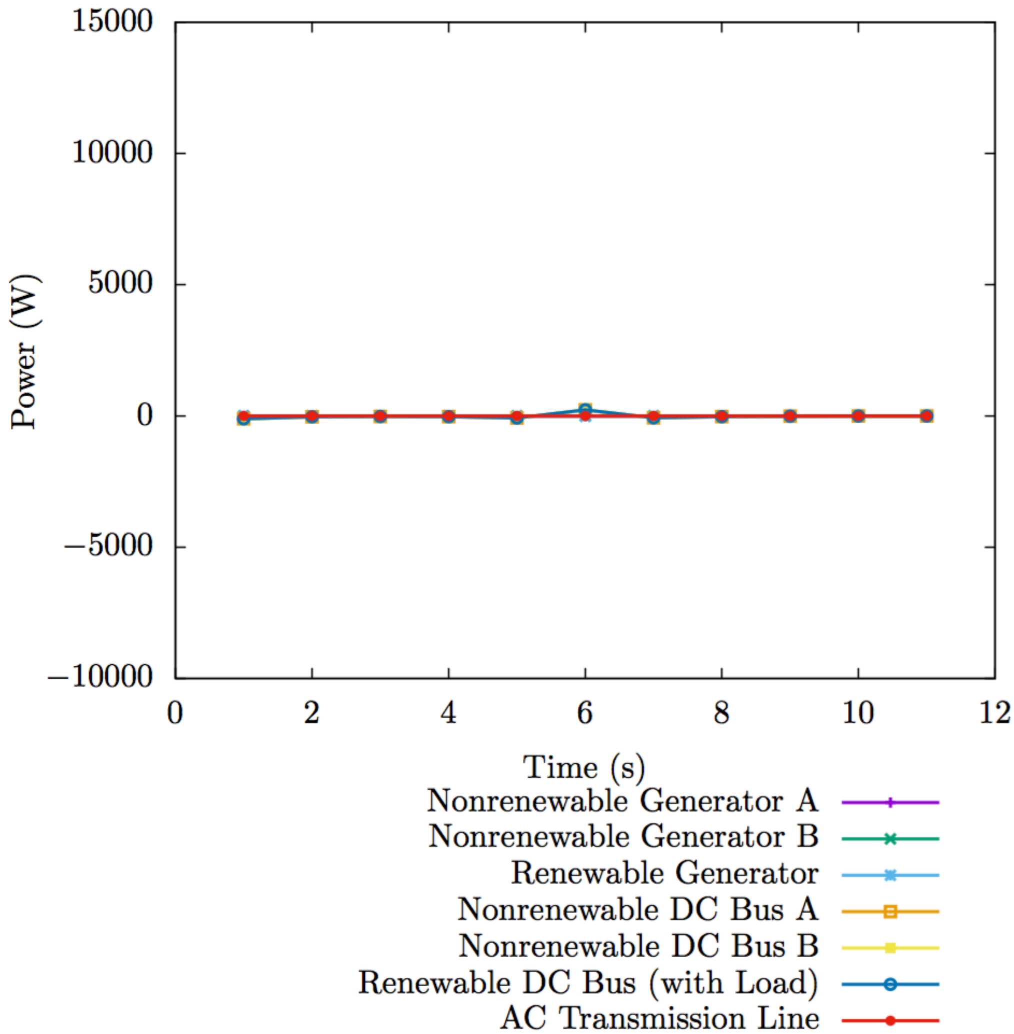

Figure 7. Power Generated/Used by Storage Device

The optimization algorithms solved multiple case studies with minimization of various criteria. Figures 4-6 show the microgrid performance for the case study of minimizing changes to boost converter duty cycles.

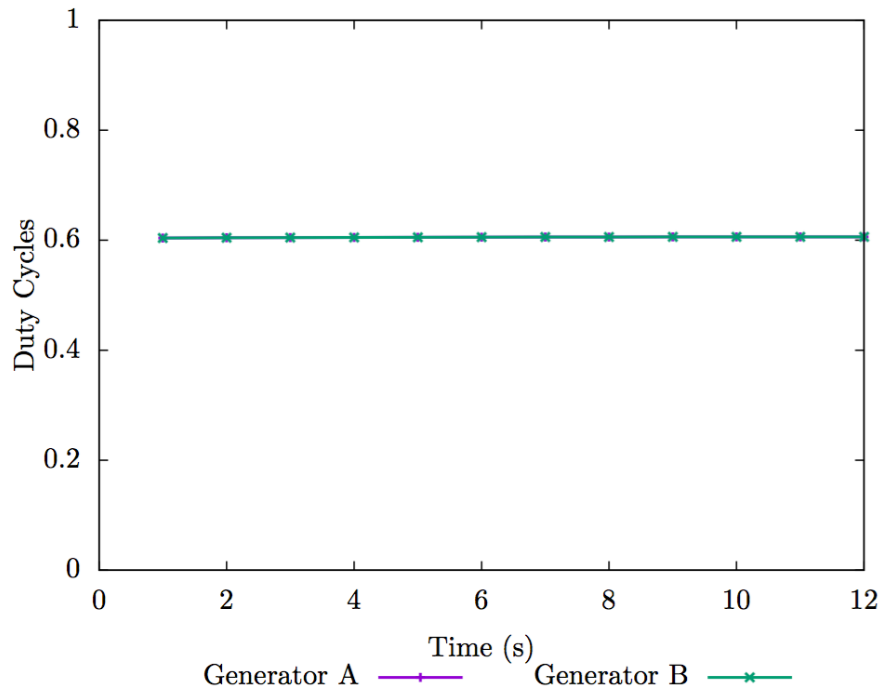

Figure 8. Boost Converter Duty Cycles

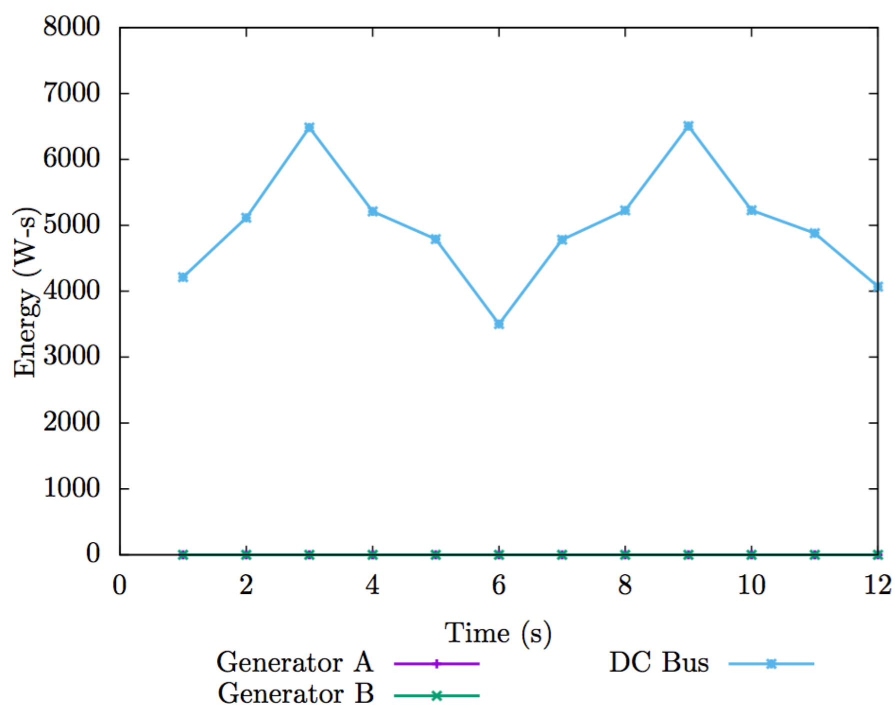

Figure 9. Energy Stored in Storage Device

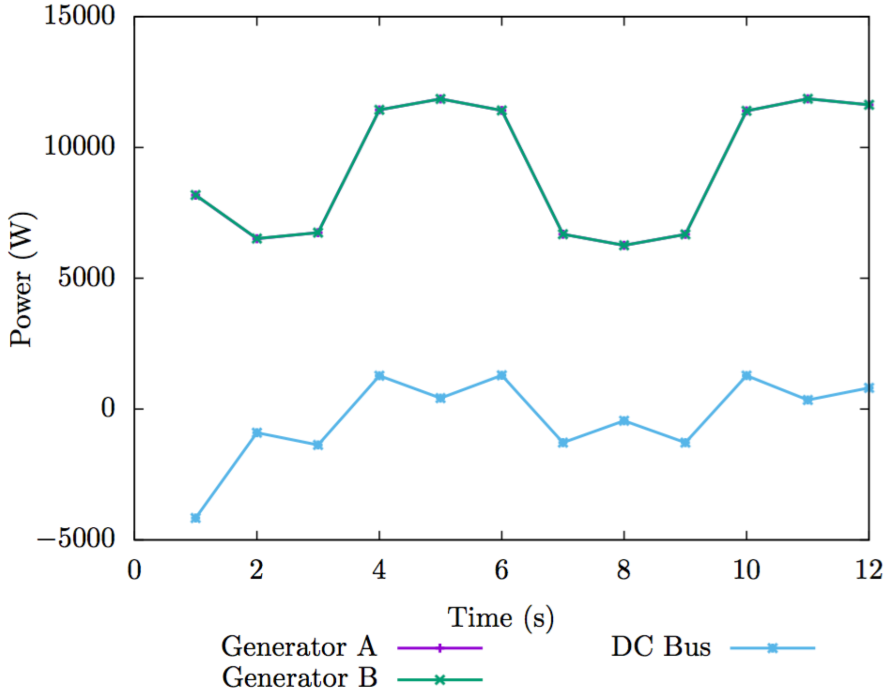

Figure 10. Power Output of Diesel Generators

5.2. HSSPFC Simulation Results

This section demonstrates the stability and verifies transient performance of the networked microgrid system with stochastic inputs. The networked AC/DC microgrid model and control analysis was performed in the Matlab/Simulink environment. Several highlights of these results are given here for discussion.

Both the input generation (representative of one varying PV input and two constant diesel generators) are tested along with a varying load profile. These profiles are shown in Figure 11 for the generator voltage input sources and for the varying load profile shown in Figure 12. The feedforward solution was updated as a function of the varying input source and load profiles (where $\tau_{ff} = 0.05$ sec). The DC bus voltage is given in Figure 13. Typical performance for DC bus voltage regulation is V_DC_nominal (plus or minus 5%).

The transient performance is improved with the tuned feedback controllers. The DC power levels for each individual microgrid are given in Figure 14 and are nominally on the order of 30kW tactical microgrid design levels. Note the PV microgrid has a higher variation in power levels. Similar results on the AC power side are shown in Figure 15 with the sum total for all three microgrids shown on the order of 90kW.

The related power requirements for each energy storage system are shown in Figure 16 along with the peak power requirement for energy storage device on DC microgrid one is shown in Figure 17 which occurs at $t = 0.4$ seconds with a magnitude of 37.5 kW. The corresponding energy storage requirements are shown in Figure 18. These profiles can be used to size the actual energy storage devices required to maintain the indicated microgrid performance shown in the other simulation results. The role of the control effort will become more evident with specific objectives and metrics (i.e., minimize fuel, energy storage charge/discharge, etc.) that will be realized through the dynamic optimization planner.

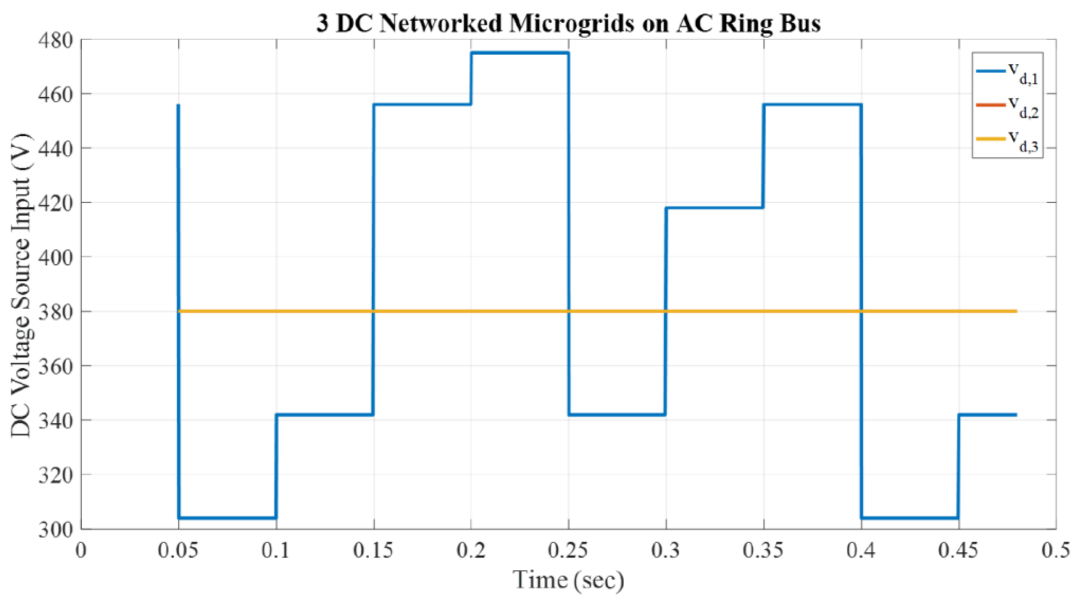

Figure 11. Variable Generator Input Microgrid 1, Constant Generator Input Microgrids 2 and 3

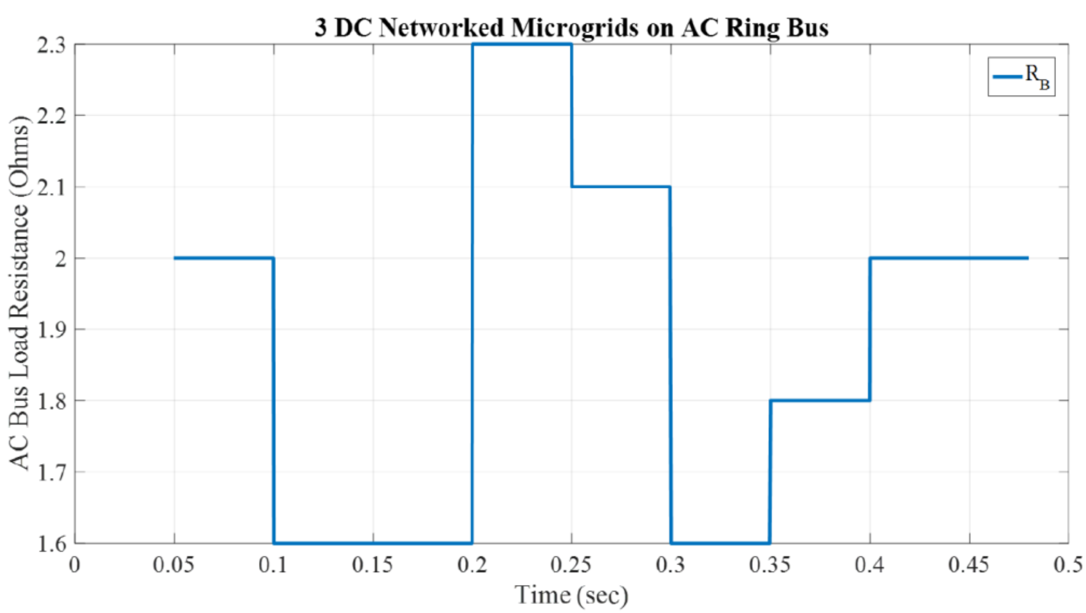

Figure 12. Variable Resistive Load on AC Ring Bus

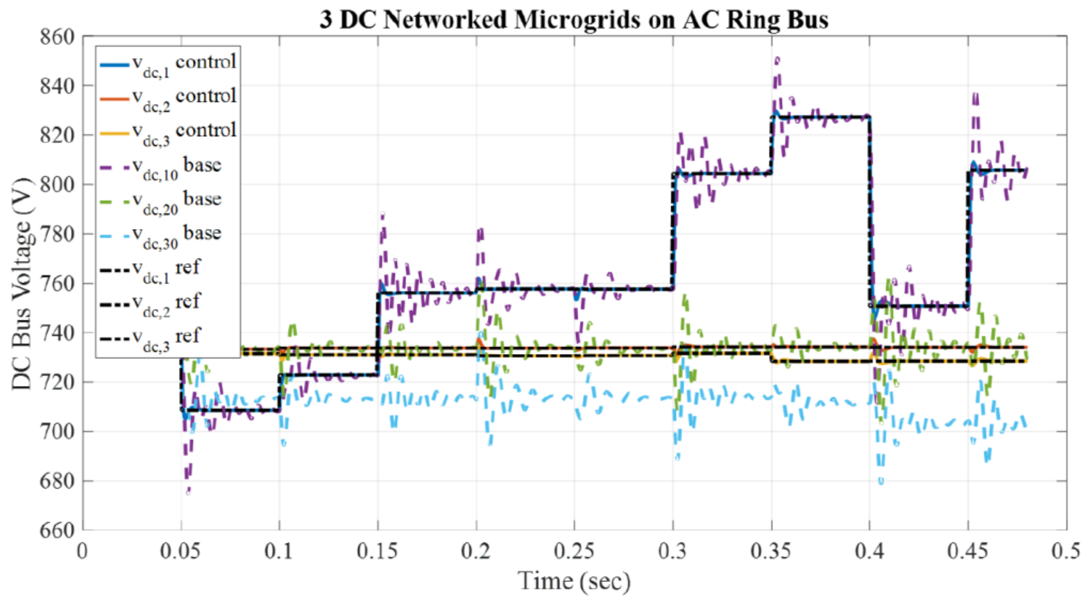

Figure 13. DC Bus Voltages with and without Controls for Each Microgrid k

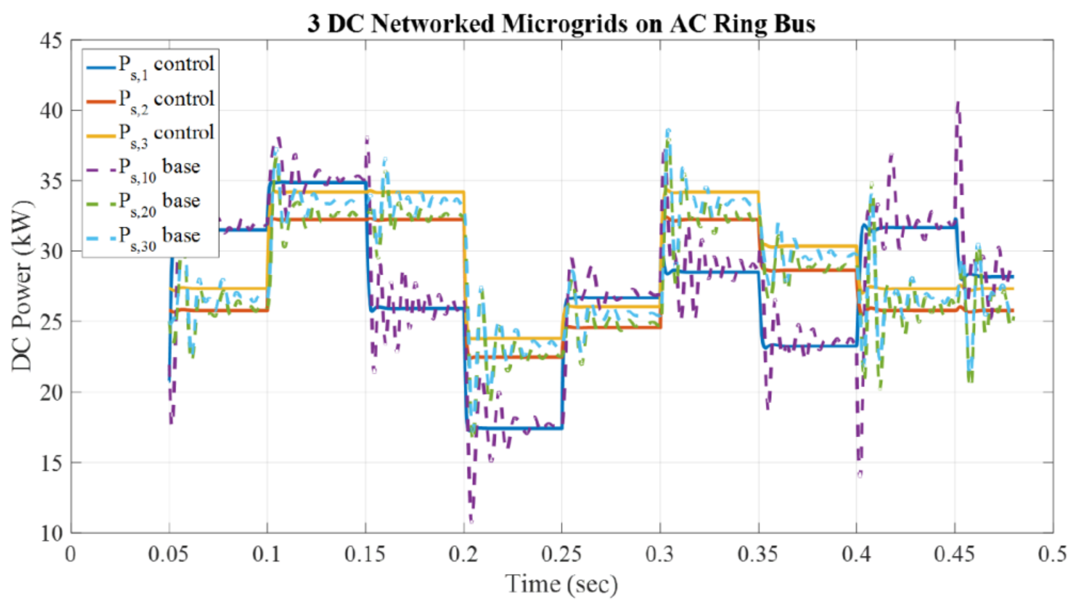

Figure 14. DC Power with and without Controls for Each Microgrid k

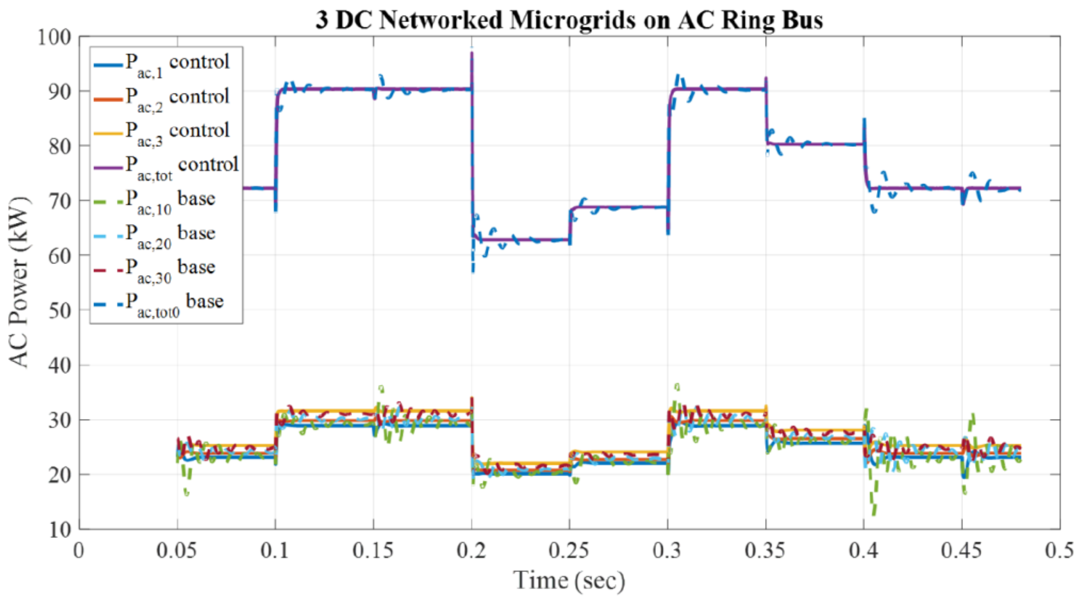

Figure 15. AC Power with and without Controls for Each Microgrid k

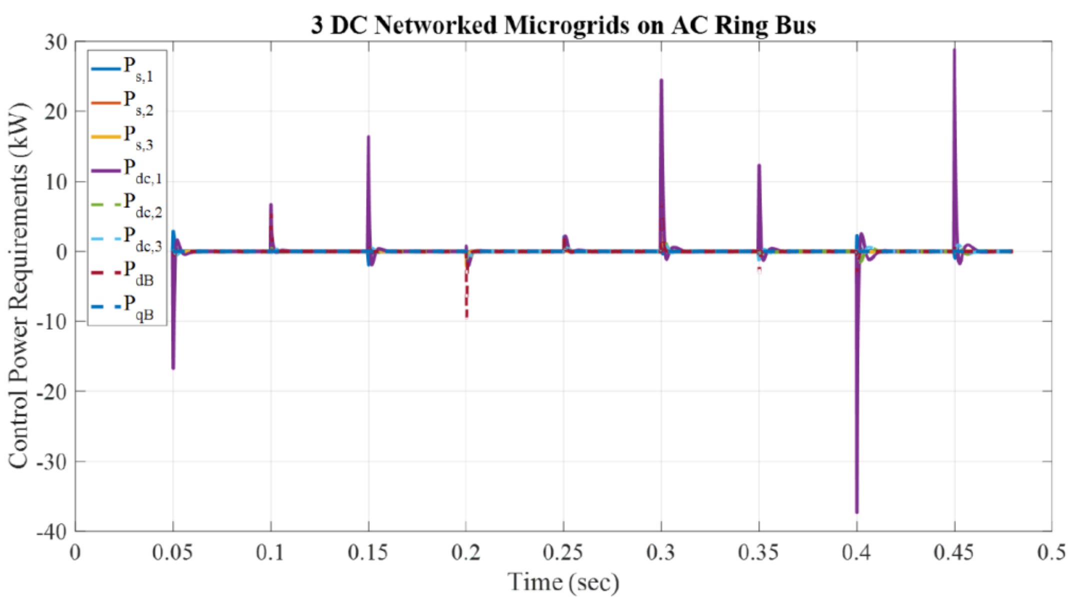

Figure 16. Control Power Requirements

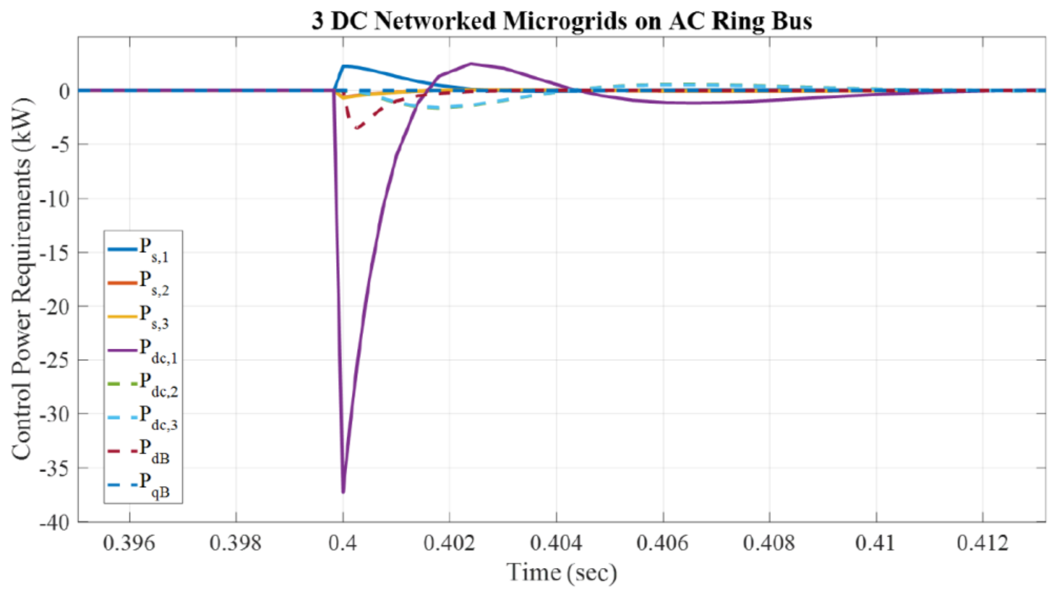

Figure 17. Control Peak Power Requirement at 0.40 seconds

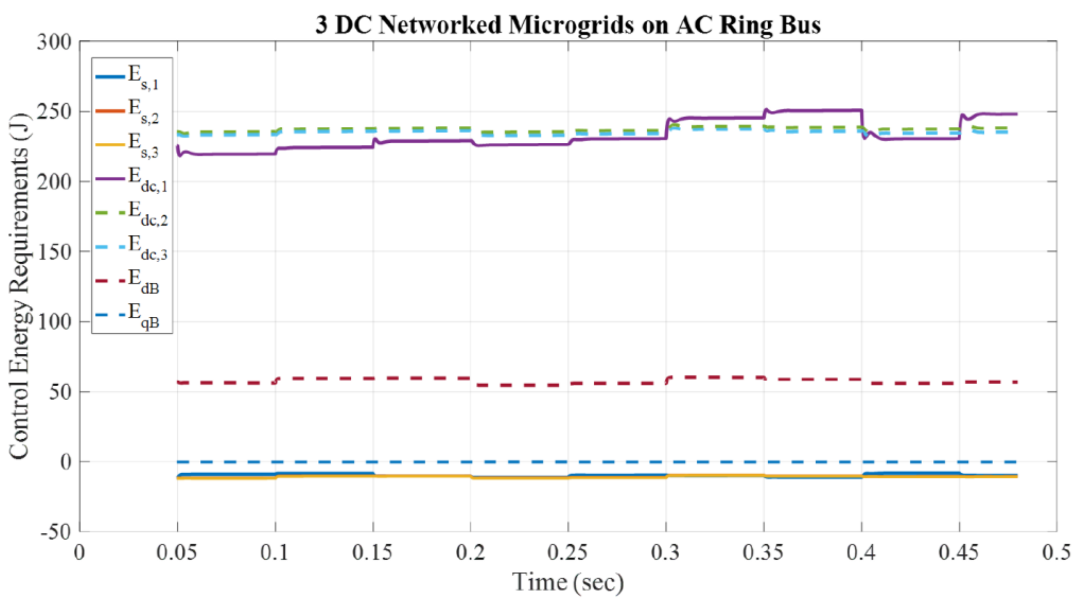

Figure 18. Control Energy Requirements

5.3. Real Time Modeling and Control Architecture

This section characterizes the algorithm implementation for real time simulations and control efforts. Sandia's custom configuration consists of a three-tier decomposition shown in Figure 19. The highest level contains the agent/informatics implementation which includes the dynamic optimization planner and can be realized on the host computer or given enough computation nodes, realized on the real-time side with a slower update rate. The next tier includes the HSSPFC feedback controller for the energy storage level that would require a quicker update rate. The lowest lever tier control contains the servo or boost/buck feedback controllers with the fastest update rate. Depending on the update rate, the servo control can be realized on the real-time side, or for quickest update rates or computation levels, at the FPGA level.

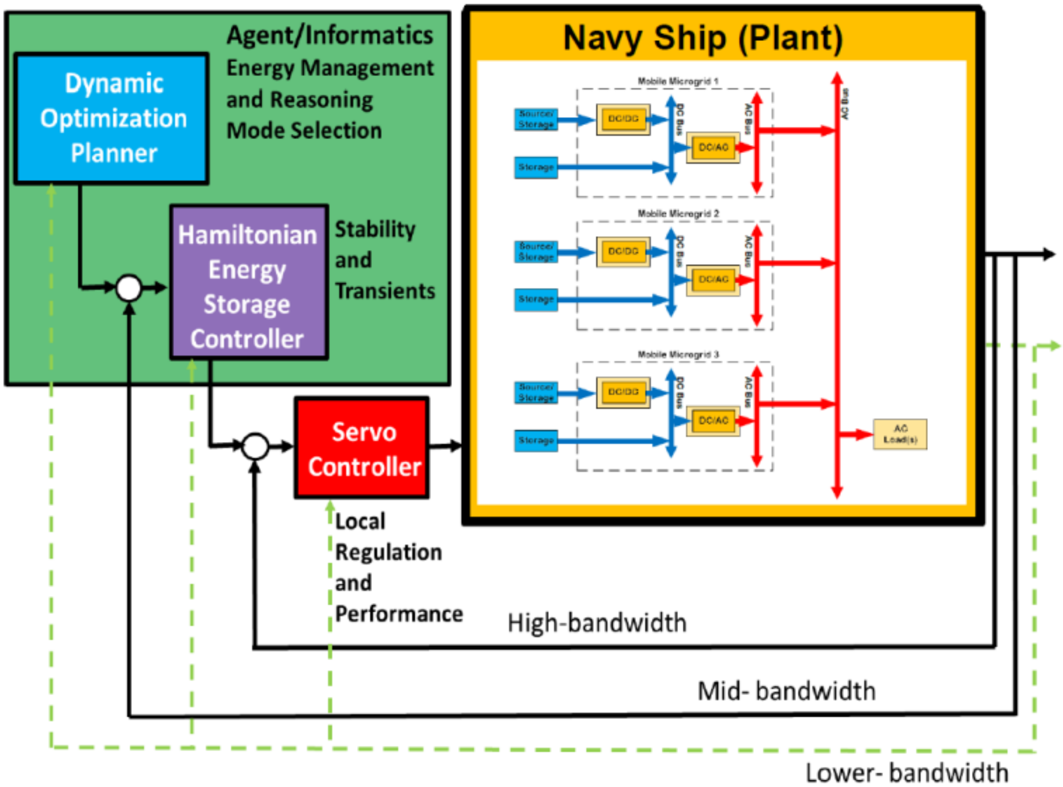

Figure 19. Three Tier HSSPFC Custom Architecture.

The network microgrid ROM model/controls pathway that was implemented in Matlab/Simulink, help to determine an efficient real-time platform partition. Figure 20 shows the component decomposition in terms of an OPAL-RT real-time simulator. The controller and networked microgrid plant model are realized on the OPAL-RT subsystem master (SM) computation node and the GUI displays and feedback information on the OPAL-RT subsystem console (SC) node.
The specific OPAL-RT RT simulator PC-based architecture is shown in Figure 21.

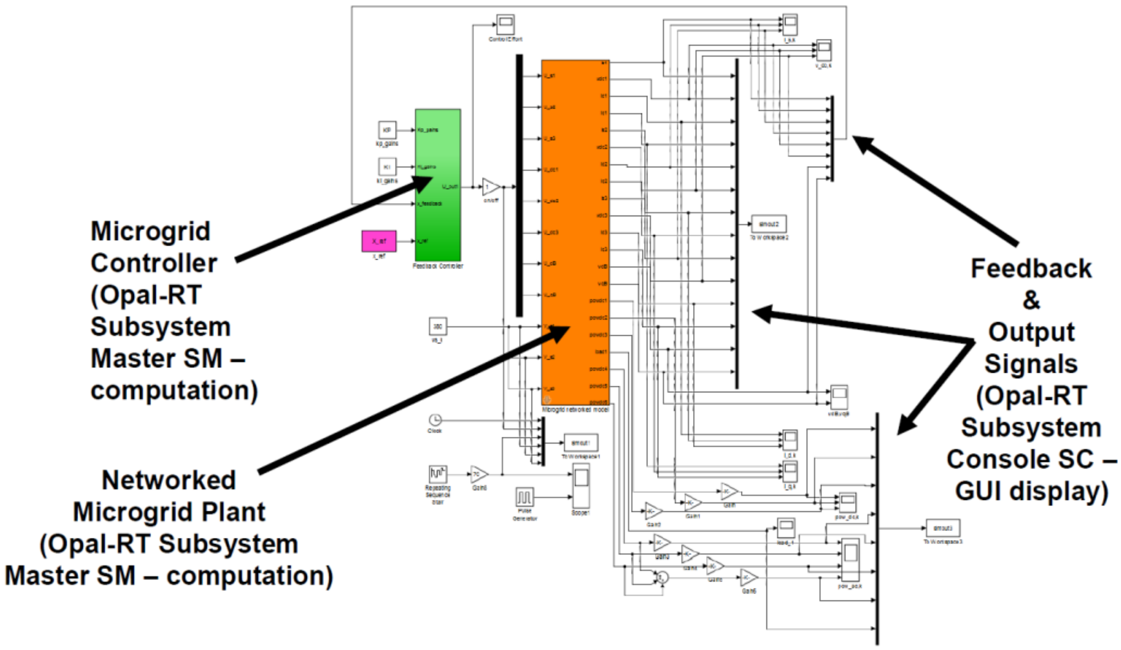

Figure 20. Networked Microgrid ROM Plant and Control Portioning for Opal-RT Target

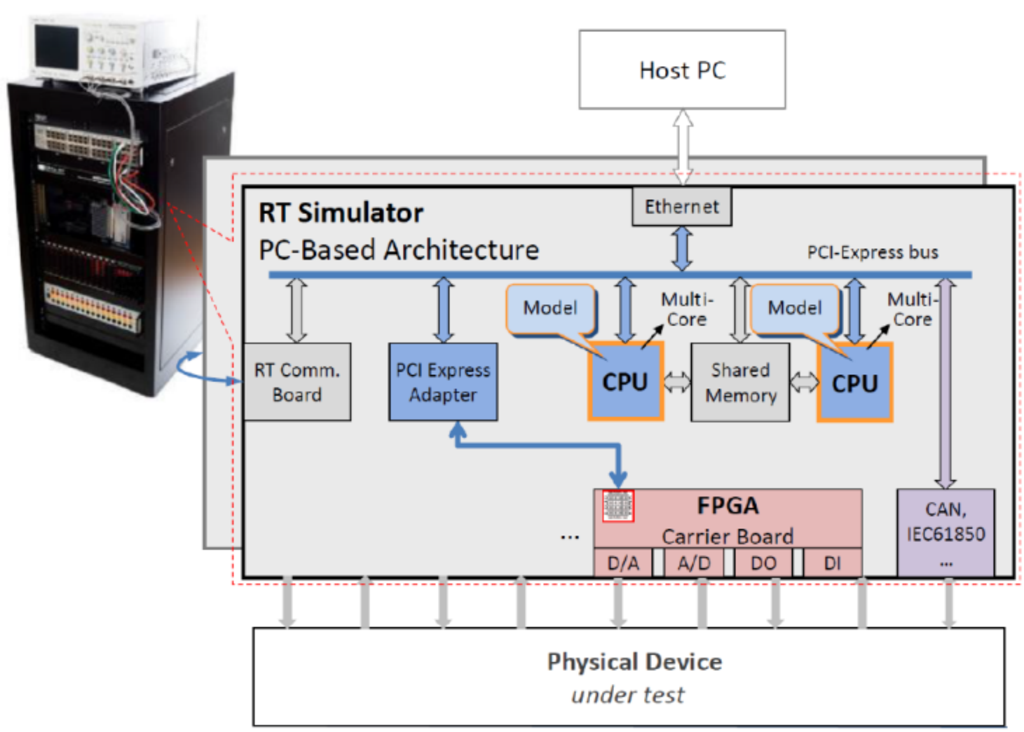

Figure 21. Opal-RT System Architecture Standard Configuration

5.4. Real-Time Microgrid Model for Advanced Control Design Studies

The thrust for the real-time high fidelity model tool [10] was to develop a single microgrid shown in Figure 22, that consisted of; i) conventional diesel (constant generation), ii) renewable energy (RE) sources, and iii) bus energy storage and loads. The objective was to have real time simulation support real-time control design. Initially, the control was characterized as an open-loop feedforward optimizer. The RE is modeled as an idealized random or periodically varying input to represent (wind, water, or solar) power generation. The model was constructed and implemented on the OPAL-RT platform with a similar as before with a computational node for the microgrid model and user interface data output node, respectively.

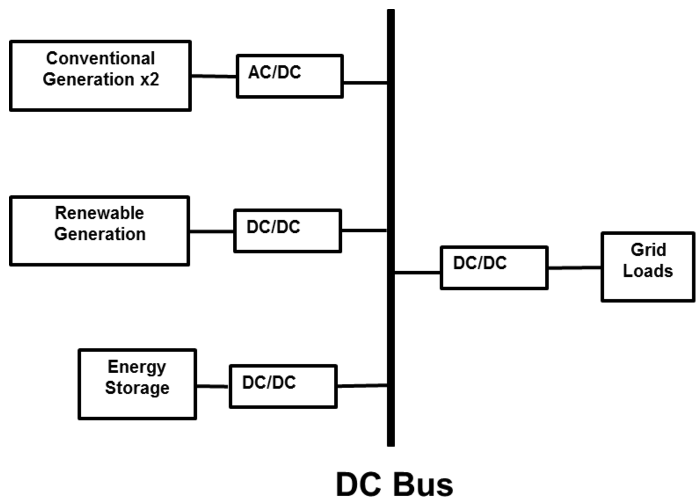

Figure 22. Single Microgrid Real Time Simulation Model

The OPAL-RT simulation oscilloscope outputs are shown in Figures 23 and 24 respectively.

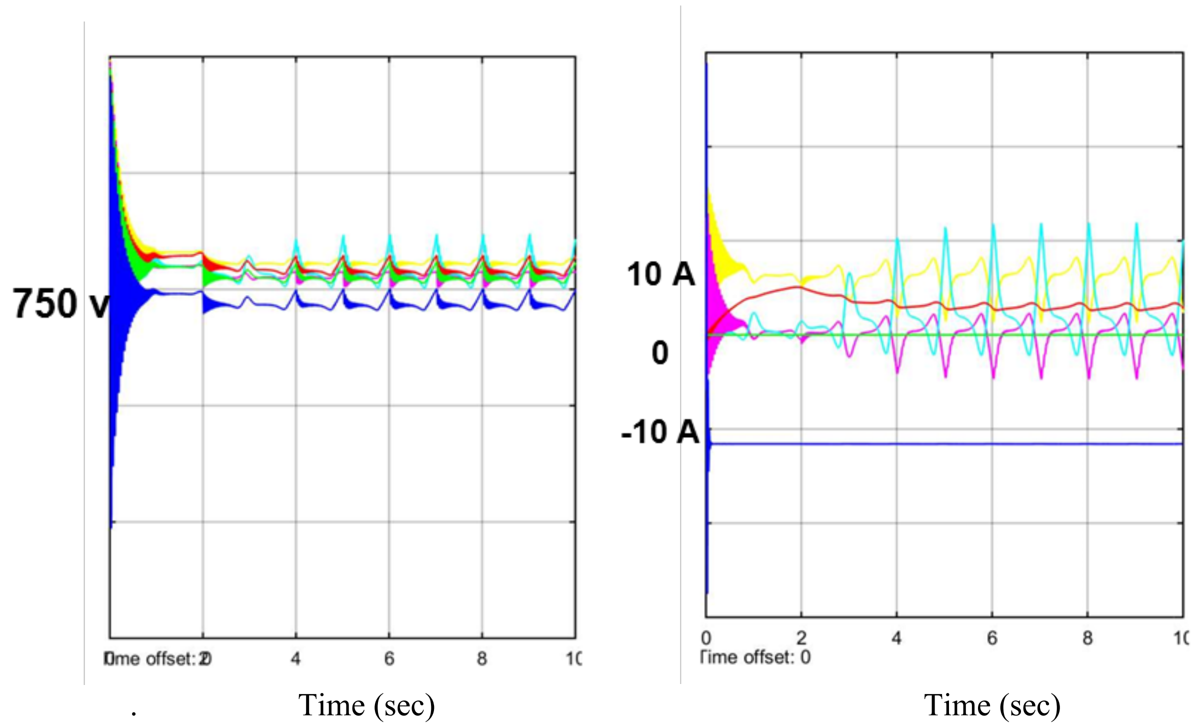

(a) (b)

Figure 23. DC Bus Voltage (a) and Source Currents (b)

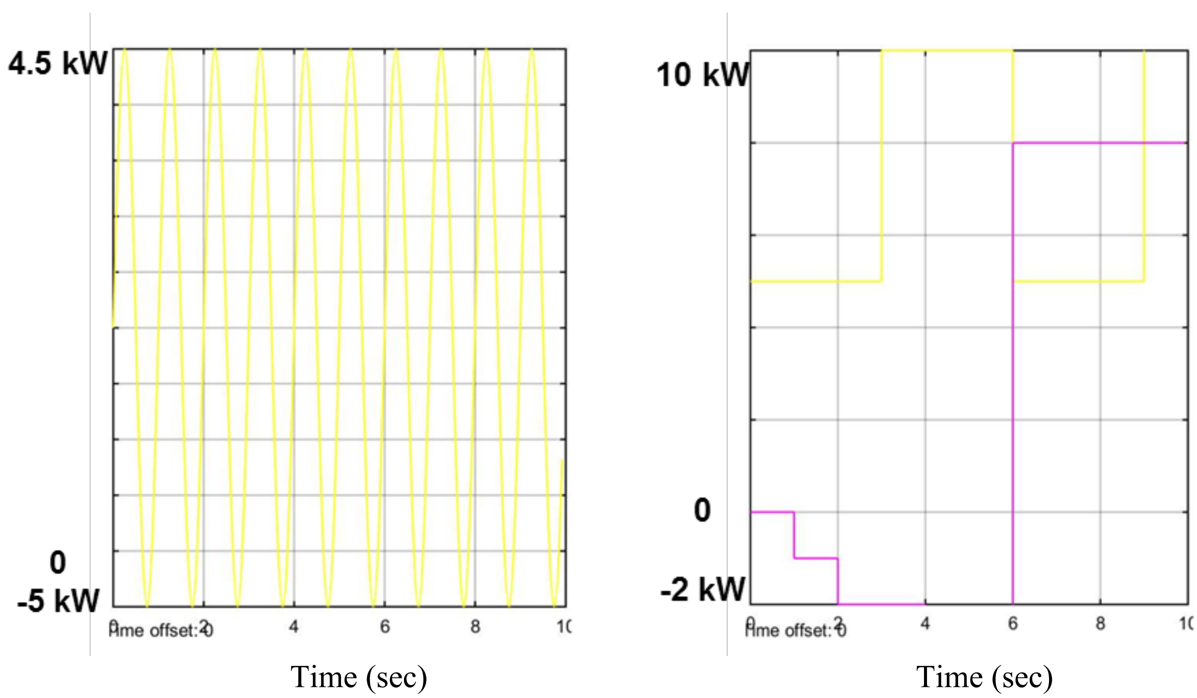

(a) (b)

Figure 24. Varying Renewable Periodic Input (a) and DC Varying Loads (b)

6. CONCLUSIONS

SNL and KIER collaborated successfully to identify hardware and simulation capabilities for networked microgrid RD&D. Controls and real time simulation with hardware in the loop capabilities were extended independently by both organizations. SNL leveraged and refined existing controls and real time simulation capabilities based on KNA campus specifications. SNL's layered control approach was leveraged to efficiently manage the KNA microgrid components. The results indicate an ability to model the energy system in both a detailed and reduced order model manner. The control performance results documented in this report indicate preliminary progress towards realizing the control architecture in a real time simulation or physical hardware environment.

REFERENCES

1. M. Cook, D. Wilson, *Experimental and Real Time Simulation*, SmartGrid_SNL_16872.pdf, Sandia National Laboratories, Albuquerque, NM, September 2017.

2. R. D. Robinett III and S. G. Glover, "Enabling Secure Scalable Microgrids with High Penetration Renewables," *Grand Challenge, LDRD, Sandia Technical Report,* SAND2011-0935P, 2011.

3. Wilson, D.G., Robinett III, R.D., Weaver, W.W., Byrne, R.H., and Young, J., Nonlinear Power Flow Control Design of High Penetration Renewable Sources for AC Inverter Based Microgrids, *International Symposium on Power Electronics, Electrical Drives, Automation and Motion*, SPEEDAM 2016, AnaCapri, Capri Island, Italy.

4. W. W. Weaver, R. Robinett III, G. Parker and D. Wilson, "Hamiltonian Modeling and Control of AC Microgrids with Spinning Machines and Inverters," *International Symposium on Power Electronics, Electrical Drives, Automation and Motion, SPEEDAM 2016,* AnaCapri, Capri Island, Italy. 2016.

5. Hassell, T., Weaver, W.W., Robinett III, R.D., Wilson, D.G., and Parker, G.G., Modeling of Inverter Based AC Microgrids for Control Development, *2015 IEEE Multi-Conference on Systems and Control*, Novotel Sydney Manly Pacific, Sydney, Australia, September 21-23, 2015.

6. Wilson, D.G. Neely, J., Cook, M., Glover, S., Young, J., and Robinett III, R.D., "Hamiltonian Control Design for DC Microgrids with Stochastic Sources and Loads with Applications," *SPEEDAM 2014,* Ishcia, Italy, 2014.

7. Wilson, D., Robinett III, R., and Goldsmith, S., "Renewable Energy Microgrid Control with Energy Storage Integration," *21st SPEEDAM 2012,* Sorrento, Italy, June 20-22, 2012

8. Robinett III, R.D. and Wilson, D.G., Nonlinear Power Flow Control Design: Utilizing Exergy, Entropy, Static and Dynamic Stability, and Lyapunov Analysis, Springer-Verlag London Ltd., August 2011, ISBN 978-0-85729-822-5.

9. J. Young, Optizelle, Open Source Optimization Software, 2016 OptimoJoe, http://www.optimojoe.com/products.optizelle

10. R. Matthews, High Fidelity Networked Microgrid Modeling SoftwareTool, User Manual, Version 3, Michigan Technological University, June 2017.

APPENDIX A: KNA CAMPUS POWER CONSUMPTION

1. Description of data acquisition in KNA campus

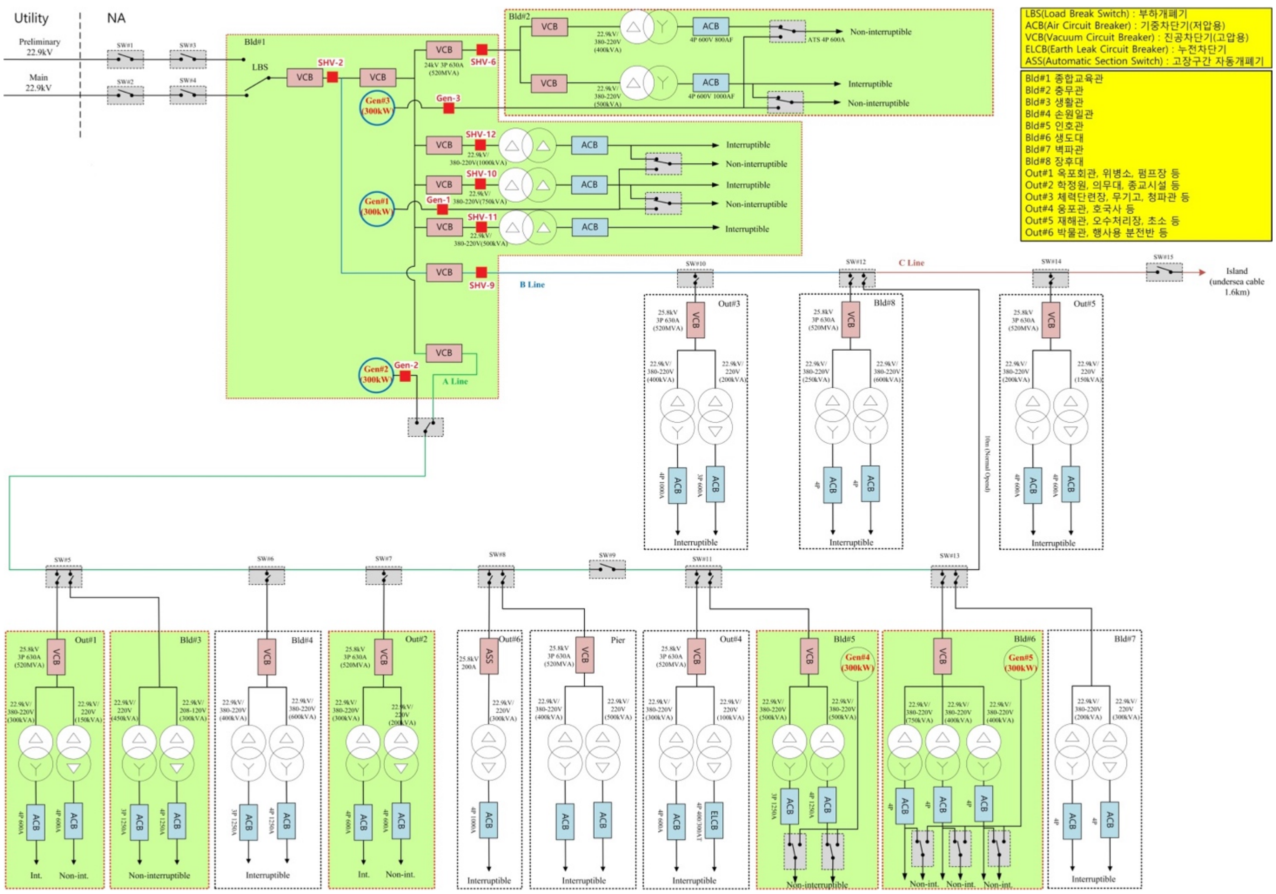

- The power meters to measure power consumption in KNA campus are SHV-2, SHV-6, SHV-9, SHV-10, SHV-11 and SHV-12

- SHV-2 measures the power consumption of whole KNA campus and a small island in the front sea which is not belong to KNA

- SHV-6 measures building #2

- Summation of the measured data of SHV-10, SHV-11 and SHV-12 produces the power consumption of building #1

- SHV-9 measures the power consumption by Out#3, Building #8, Out #5 and an island

- The power provided to A-line are calculated by SHV-2 - (SHV-9 + SHV-10 + SHV-11 + SHV-12), but the power provided to Out #1, Building #3, Out #2, Pier, Building #5 and Building #6 of A-line are not measured separately, which are critical loads.

2. Data files(: MB.zip)

1) The data files, “MB_Power_xxxx” of “MB.zip”, are measured data every 10 second from June. 2016 to May. 2017

- Unit of Y axis is kW

- The first column of MB_Power_xxxx, KNA all, is calculated by SHV-2 – SHV-9. Since SHV-9 measures the power consumption by Out#3, Building #8, Out #5 and an island, the first column does not show the power consumption of whole KNA campus exactly, which is a little bit less.

- The second column of MB_Power_xxxx, BLDG1, is calculated by SHV-10 + SHV-11 + SHV-12

- The third column of MB_Power_xxxx, BLDG2, is the measured data by SHV-6

- The fourth column of MB_Power_xxxx, A line, is calculated by SHV-2 - (SHV-9 + SHV-10 + SHV-11 + SHV-12)

2) The data files, MB_Eng_xxxx are calculated using MB_Power_xxxx, whose Y axis unit is kWh

3. Figures

1) The first column of MB_Power_xxxx

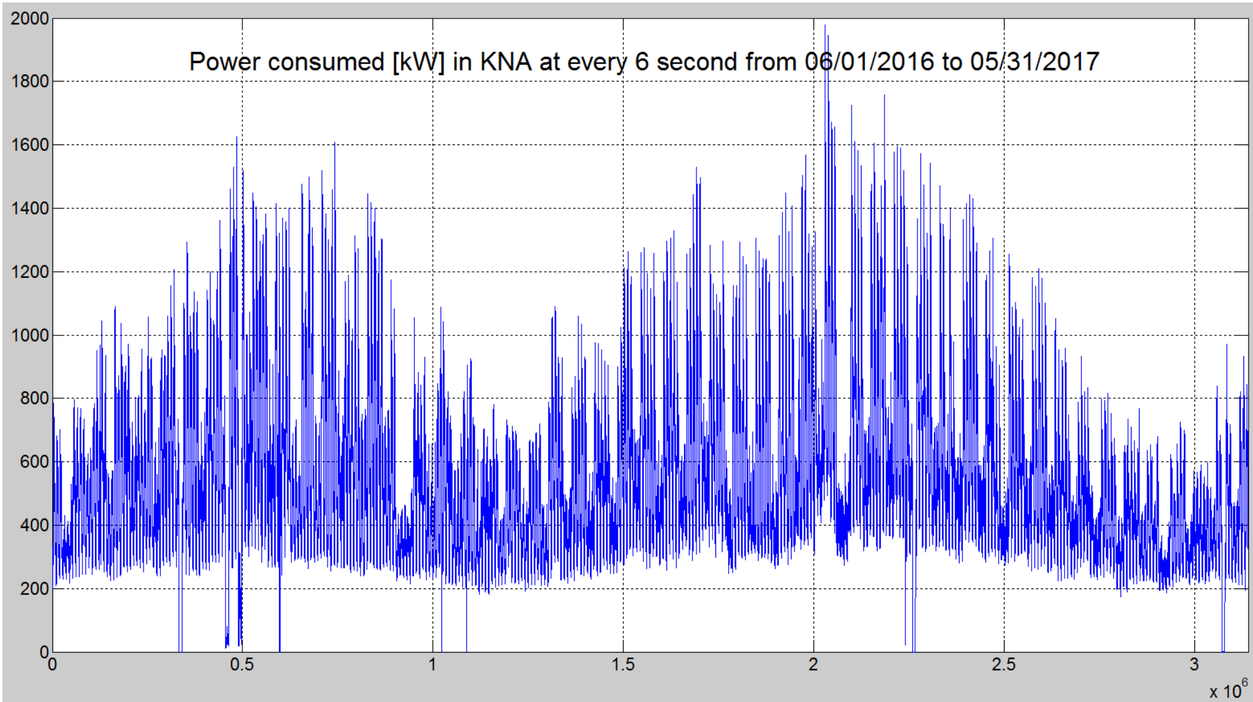

- Unit of X axis is X x 10sec (6 second on the figure is error). The last number of X axis is 3141037 which means about 1 year because (3141037 x 10sec)/3600/24=364 days
- Unit of Y axis is kW

2) The first column of MB_Eng_xxxx

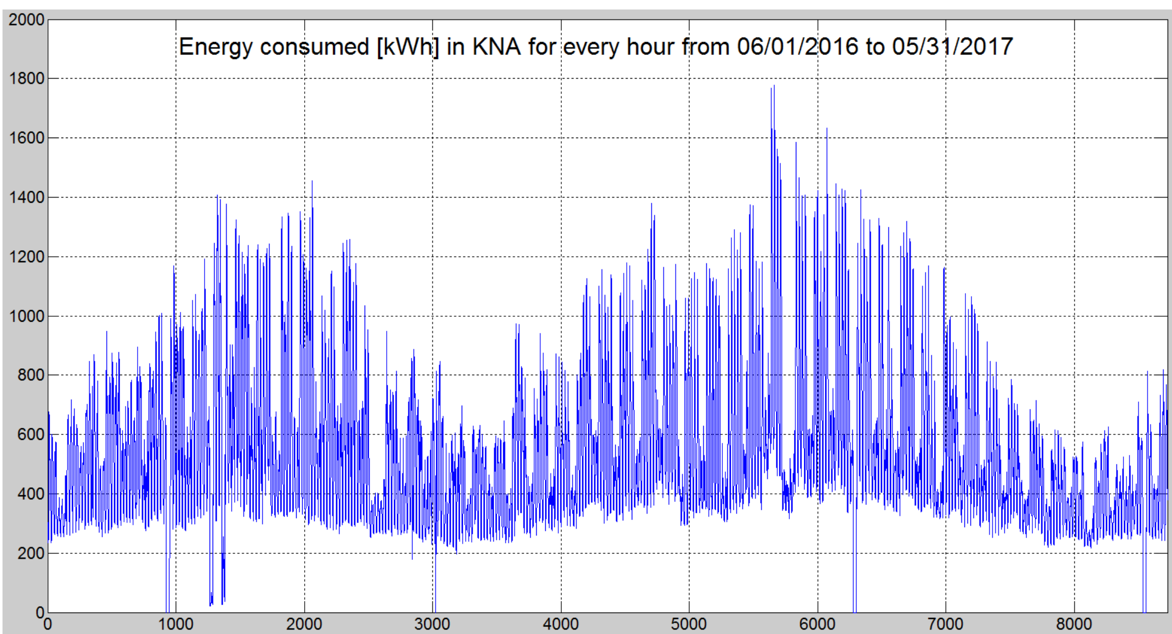

- Unit of X axis is hour. The last number of X axis is 8725 which means about 1 year data because 8725/24=364 days

- Unit of Y axis is kWh

3) The second column of MB_Power_xxxx

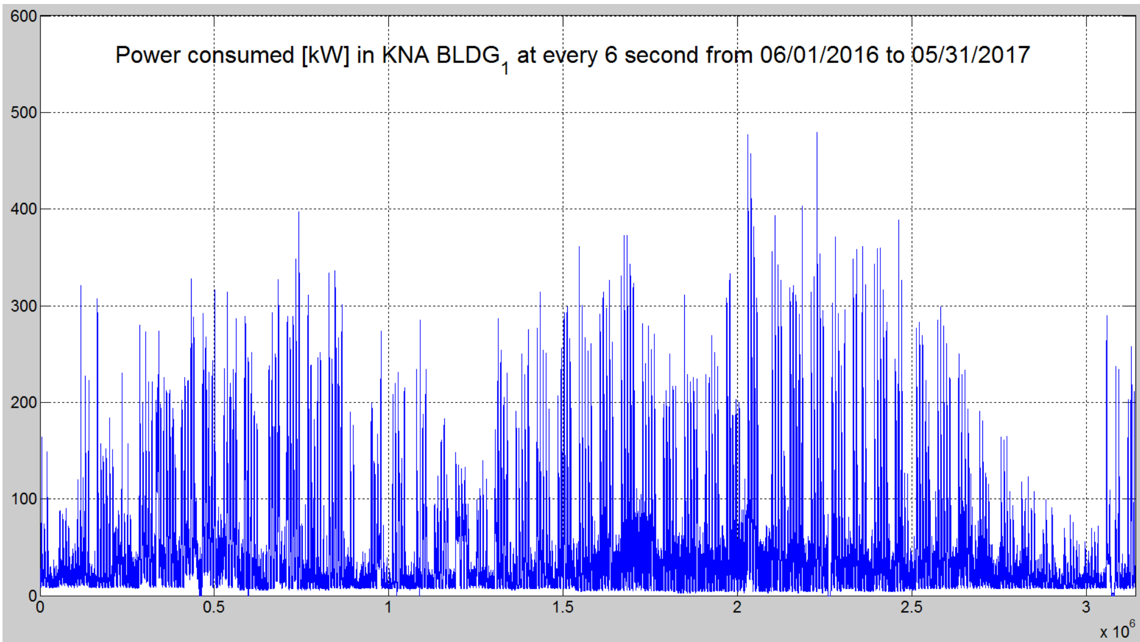

- Unit of X axis is X x 10sec
- Unit of Y axis is kW

4) The second column of MB_Eng_xxxx

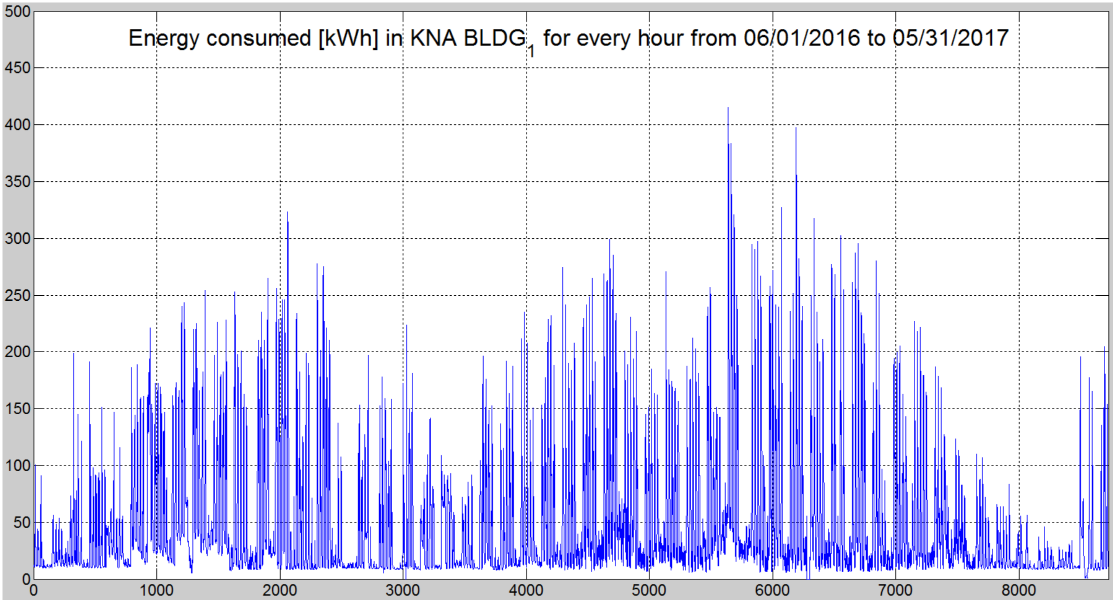

- Unit of X axis is hour.
- Unit of Y axis is kWh

5) The third column of MB_Power_xxxx

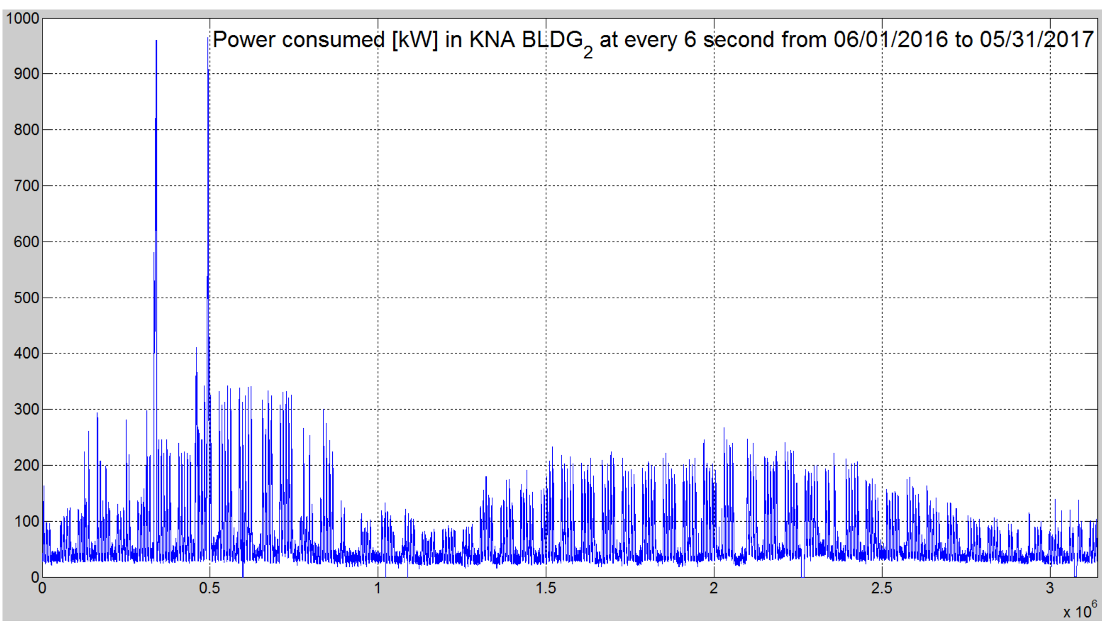

- Unit of X axis is X x 10sec
- Unit of Y axis is kW

6) The third column of MB_Eng_xxxx

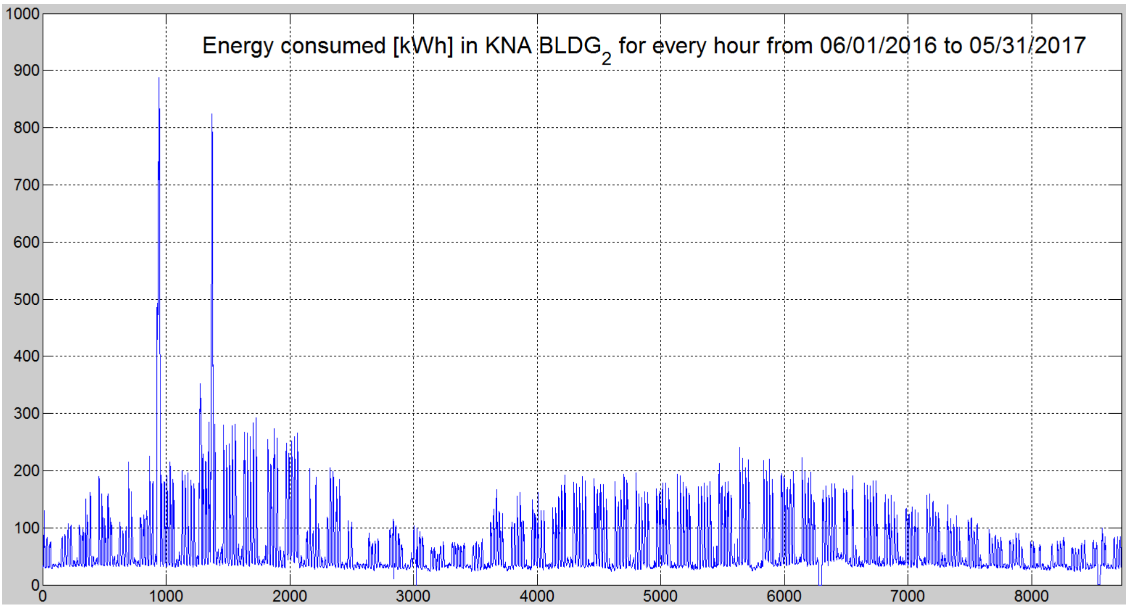

- Unit of X axis is hour.
- Unit of Y axis is kWh

7) The fourth column of MB_Power_xxxx

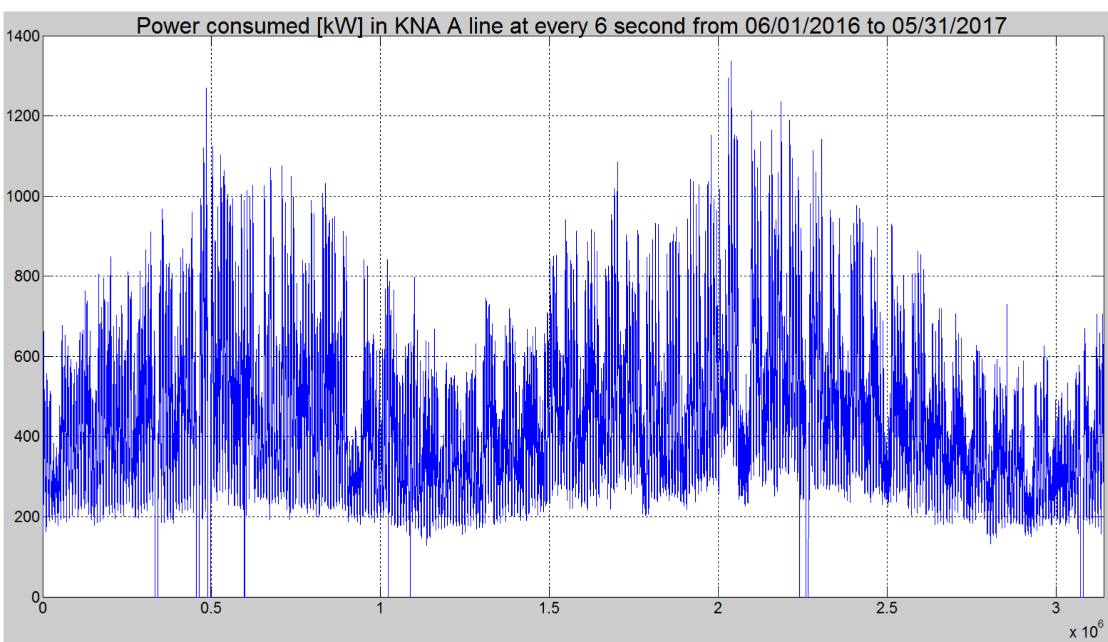

- Unit of X axis is X x 10sec
- Unit of Y axis is kW

8) The fourth column of MB_Eng_xxxx

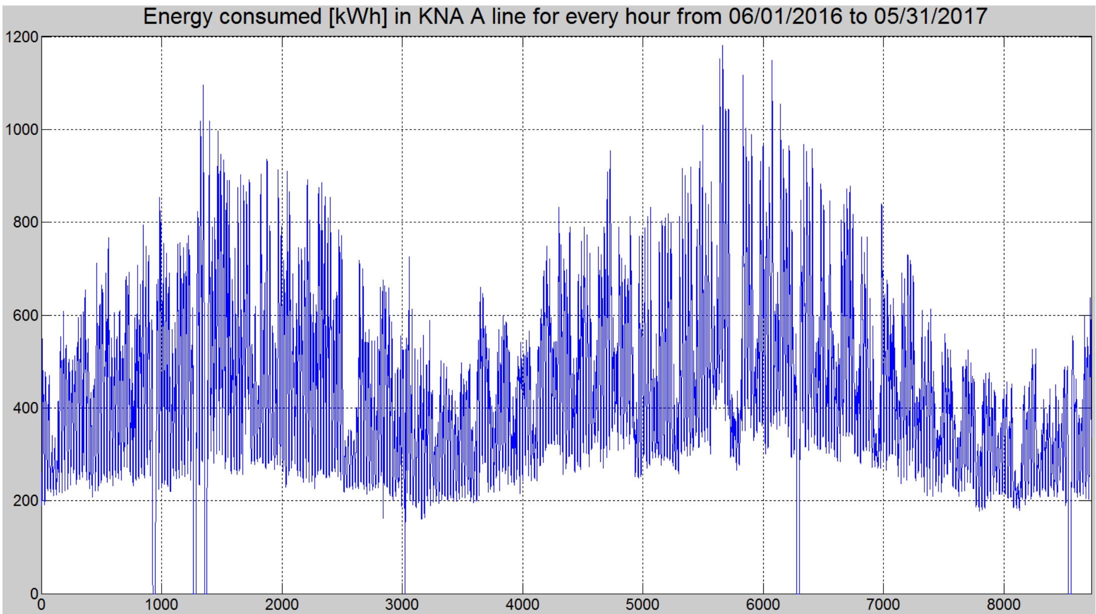

- Unit of X axis is hour.
- Unit of Y axis is kWh

DISTRIBUTION

MS1033	Abraham Ellis	08812
MS1108	Marvin Cook	08836
MS1152	David Wilson	01353

Sandia National Laboratories